

Multidimensional performance limit state for probabilistic seismic demand analysis

Xiao Xiao Liu¹ · Zi-Yan Wu¹ · Feng Liang¹

Received: 13 May 2016 / Accepted: 16 September 2016 / Published online: 26 September 2016
© Springer Science+Business Media Dordrecht 2016

Abstract Based on a framework of Probabilistic Seismic Demand Analysis, a nonlinear dynamic model of a reinforced concrete (RC) building was established to obtain a demand hazard curve that considers multidimensional performance limit states (MPLSs), including combinations of peak floor acceleration and interstory drift. A definition of the two limit states is expressed using a generalized MPLSs equation. The peak floor acceleration and the interstory drift were considered to be dependent and were assumed to follow a bidimensional lognormal distribution. The maximum interstory drift and the maximum peak floor acceleration were calculated using Increment Dynamic Analysis and nonlinear time history analysis. The numerical formula for a demand hazard curve of the modelled building was then derived by coupling the bidimensional lognormal distribution with the ground motion hazard curve. The uncertainties involved in MPLSs and structural parameters, as well as the different threshold values for peak floor acceleration, were further considered to determine the sensitivity of demand hazard curves. The analysis results showed that the proposed method can be used to describe the damage performance of various building structures, which are sensitive to multiple response parameters including drift and acceleration. Moreover, it was demonstrated in this study that the demand hazard curves were relatively conservative if the coefficient of variation, the peak floor acceleration threshold, the interaction factor N_{IDR} and added stiffness, were appropriately selected.

Keywords Probabilistic seismic demand analysis · Demand hazard curve · Multidimensional performance limit states · Bidimensional lognormal distribution · Seismic hazard curve

✉ Xiao Xiao Liu
xxliu1989@163.com

¹ Department of Civil Engineering, Northwestern Polytechnical University, Dist. Chang'an, Xi'an 710129, China

Abbreviations

MPLSs	Multidimensional performance limit states
IDA	Incremental Dynamic Analysis
PSDA	Probabilistic Seismic Demand Analysis
PSHA	Probabilistic seismic hazard analysis
EDP	Engineering Demand Parameter
PDF	Probability density function
<i>IDR</i>	The maximum interstory drift
<i>PFA</i>	The maximum peak floor acceleration
<i>IM</i>	Intensity measures
$S_a(T_1)$	Spectral acceleration
<i>idr</i>	Threshold value of the interstory drift limit state
<i>pfa</i>	Threshold value of the peak floor acceleration limit state
idr_{lim}	Interstory drift limit state
pfa_{lim}	Peak floor acceleration limit state
$idr_{rand\ lim,i}$	A random threshold value of the interstory drift limit state at the <i>i</i> th performance level
$pfa_{rand\ lim,i}$	A random threshold value for the peak floor acceleration limit state at the <i>i</i> th performance level
$idr_{fixed\ lim,i}$	A deterministic threshold value of the interstory drift limit state at the <i>i</i> th performance level
$pfa_{fixed\ lim,i}$	A deterministic threshold value for the peak floor acceleration limit state at the <i>i</i> th performance level
$idr_{lim,ij}$	A deterministic interstory drift limit state at the <i>i</i> th performance level
$pfa_{lim,j}$	The <i>j</i> th fixed peak floor acceleration limit state
ε	Uncertainties of ground motion and epistemic uncertainty
Y	Uncertainties of structural system characteristics
N_{IDR}, N_{PFA}	Interaction factor determining the shape of the surface of 2D limit state
Ω	The one-dimensional failure domain of the structure
D	The two-dimensional failure domain
$\mu_{IDR IM=im}$	The log-mean of interstory drift
$\sigma_{IDR IM=im}$	The log-standard deviation of interstory drift
$\mu_{PFA IM=im}$	The log-mean of peak floor acceleration
$\sigma_{PFA IM=im}$	The log-standard deviation of peak floor acceleration
ρ	The correlation coefficient
cv	The coefficient of variation
$f(IDR, PFA IM = im)$	PDF of a bivariate lognormal distribution
$f(IDR)$	PDF of the interstory drift
$f(idr_{rand\ lim,i})$	PDF of interstory drift limit state
$P(IDR > idr IM = im)$	The hazard fragility function

$P(IDR > idr, PFA > pfa IM = im)$	A two-dimensional hazard fragility function
$\lambda_{IM}(im)$	Seismic hazard function of the site originated from PSHA
$v_{IDR}(idr)$	The mean annual frequency of exceeding the interstory drift limit state
$v_{IDR,PFA}(idr, pfa)$	The mean annual frequency of exceedance that includes two limit states
$v_{IDR}(idr_{rand\ lim,i})$	The mean annual frequency of exceeding the random interstory drift limit state
$v_{IDR,PFA}(idr_{lim,ij}, pfa_{lim,j})$	The mean annual frequency of exceeding i th fixed interstory drift limit state when the effect of j th acceleration threshold is considered
$v_{IDR,PFA}(idr_{rand\ lim,i}, pfa_{rand\ lim,i})$	The mean annual frequency of exceeding two randomly independent/interdependent limit states
$P[idr < IDR(Y = y, IM, \varepsilon)]$	The probability of structural damage in the design working life
$P[idr < IDR(Y = y, IM, \varepsilon), pfa]$	The probability of structural damage that reflects two performance limit states
$P[idr_{lim,ij} < IDR(Y = y, IM, \varepsilon), pfa_{lim,j}]$	The probability of structural damage when the effect of j th acceleration threshold is considered

1 Introduction

Recent devastating natural hazards have caused structural damages and great economic losses in a number of countries. Excessive deformation often leads to severe damage to building structural members, but traditional force-based design methods underestimate the deformation of the damaged components. Therefore, force-based designs have been unable to meet earthquake-resistant requirements (Priestley 2000; Ghobarah 2001). Many foreign and domestic scholars have begun to investigate a new seismic design method. In this regard, American investigators have been the first to shift from force-based to performance-based or displacement-based seismic design. Presently, performance-based design, which emphasizes multi-level and multi-target fortifications, has become the developmental trend in seismic design in the worldwide construction industry. Due to the uncertainties of ground motion parameters and structural materials, structural responses are usually considered as uncertain. Many academics have suggested that probabilistic term should be the basis for discussion of the philosophy and methods of performance-based seismic design (Porter 2003; Deierlein et al. 2003; Moehle and Deierlein 2004). In particular, the U.S. Pacific Earthquake Engineering Research (PEER) Center has presented a framework for performance-based earthquake engineering (PBEE), which was established using full probabilistic theory (Deierlein, et al. 2003; Moehle and Deierlein 2004). One goal of PBEE has been to calculate the mean annual frequency of surpassing a given level of structural response. Consequently, some experts have utilized Probabilistic Seismic Demand Analysis (PSDA) to calculate the mean annual exceeding frequency and evaluate the seismic performance level of structures that will be subjected to a future earthquake event (Tothong 2007; Shome 1999). The ultimate aim of PSDA is to obtain a structural demand hazard curve based on a multi-performance level, which would be similar to the seismic hazard curve obtained using the Probabilistic Seismic Hazard Analysis (PSHA)

(Cornell 1968). A notable work (Yun et al. 2002) has evaluated the seismic performance of steel-frame structures at two performance levels using PSDA. Other recent studies (Tothong and Cornell 2006; Zeng et al. 2012; Wu et al. 2012) have shown that the demand hazard curves of building structures and bridges can be developed by combining PSDA with Incremental Dynamic Analysis (IDA).

Although these efforts have focused on the evaluation of structural demand hazards (e.g., drift hazard, bearing displacement hazard, etc.) at various performance levels, the literature reviewed in the introduction to this paper are by no means comprehensive. For example, the performance limit threshold is viewed only as a deterministic quantity in PSDA, whereas it is intended to be regarded as a random variable. Furthermore, in the PSDA analysis either a single performance limit state is employed or two unrelated limit states are used in the analysis. By contrast, outstanding researches (Cimellaro et al. 2006; Cimellaro and Reinhorn 2010) have emphasized that structural seismic performance should be estimated using bidimensional performance limit states (e.g., drifts, accelerations, etc.). In addition, similar application investigations have also been reported in the literature that focus on improving the accuracy of seismic performance evaluation (Wang et al. 2012; Sun et al. 2013). However, the dependencies between multiple demand parameters and the application of the seismic fragility have not been addressed in these reported studies. In addition, to date there have been few literature reports of how multiple limited parameters affect structural demand hazards. The study reported here maintains that the demand hazard curves of a given structure should be evaluated using two different types of seismic demands. To be realistic, the uncertainties of two limit states and the dependencies between two responses were combined to develop demand hazard curves for a structure.

An effective methodology for calculating structural demand hazards is presented in this study by considering bidimensional performance limit states. The proposed method was then applied to a six story RC frame structure, selecting the peak floor acceleration and the interstory drift as Engineering Demand Parameters (EDPs). Four performance levels of the modelled building were defined based on the strength of the combination of the performance of various structural components (ATC58-2 2006). The corresponding limit states were defined using a generalized MPLSs equation. Subsequently, the maximum interstory drift and the maximum peak floor acceleration were calculated using Increment Dynamic Analysis and nonlinear time history analysis. Since the two seismic responses follow a bidimensional lognormal distribution, the demand hazard curves of the modelled building were derived by combining the bidimensional fragility curve and the seismic hazard curve. To increase the conservative nature of the demand risk assessment, the uncertainties of limit states, structural parameters and peak floor acceleration thresholds were discussed based on the sensitivity analysis of demand hazard curves.

A framework of the proposed technical process is presented in Fig. 1.

2 Probabilistic seismic demand analysis (PSDA)

2.1 Performance-based PSDA

PSDA can predict the structural responses that will occur in future earthquakes using probabilistic methods. These predictions are then used to evaluate the seismic performance of structures by combining the results with probabilistic seismic hazard analysis (PSHA). In this reported study, following the PEER practice, a structural response can be termed an

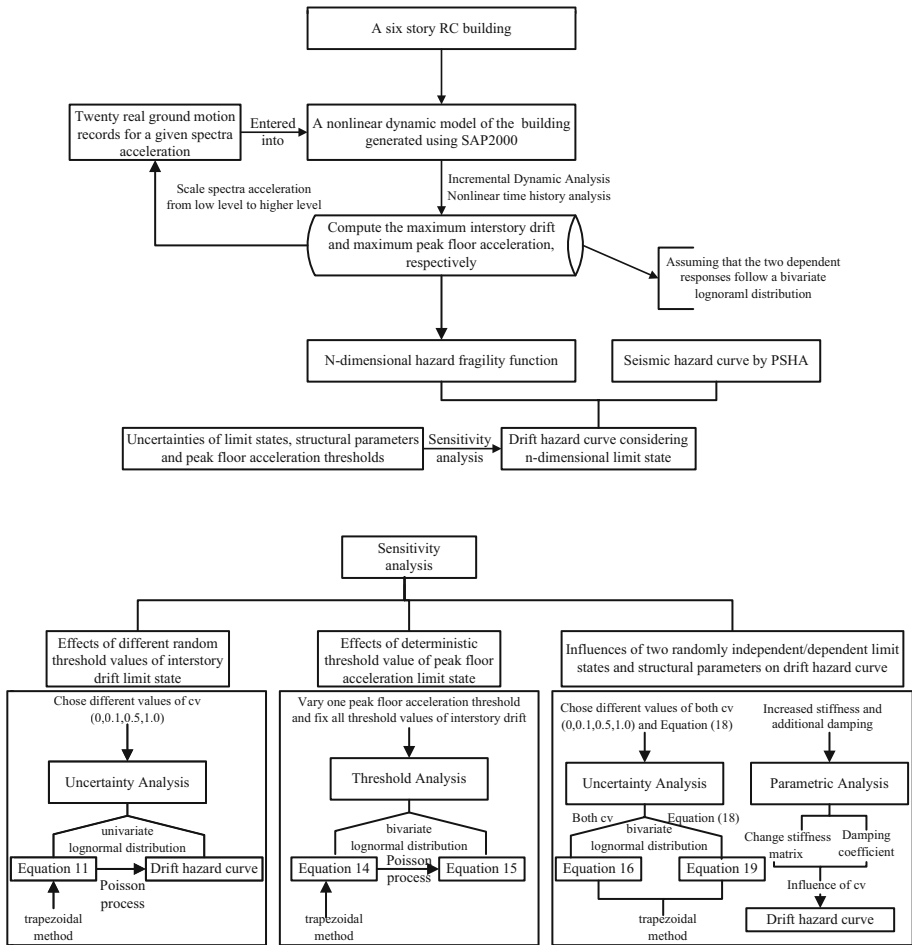


Fig. 1 Flowchart of the proposed methodology

Engineering Demand Parameter (EDP) and can be computed using IDA (Vamvatsikos and Cornell 2004). The intensity of a ground motion record is represented by an intensity measure (*IM*), which might be represented by a spectral acceleration or peak ground acceleration. If the maximum interstory drift in a structure is considered to be the only EDP and the *IM* is considered to be the spectral acceleration $S_a(T_1)$, the mean annual frequency of exceeding a given limit level can be calculated (Baker and Cornell 2005; Lin et al. 2011) according to:

$$v_{IDR}(idr) = \int_{IM} P(IDR > idr | IM = im) \left| \frac{d\lambda_{IM}(im)}{dim} \right| dim \quad (1)$$

where $v_{IDR}(idr)$ is the mean annual frequency of exceeding the interstory drift limit state; *IDR* is the maximum interstory drift; *idr* is threshold value of the interstory drift limit state; *IM* is spectral acceleration; $\lambda_{IM}(im)$ is the seismic hazard function of the site originated from PSHA (Jalayer 2003). The term $P(IDR > idr | IM = im)$ represents the hazard fragility

function. From Eq. (1) it can be seen that performance-based PSDA is needed to compute a structural response and a ground motion hazard curve. This numerical integration can be calculated using a trapezoidal method.

Kiureghian (2005) revealed that the structural damage event $\{edp < EDP(y, IM, \varepsilon)\}$ was Poisson in time and a structural demand hazard function could be expressed as:

$$P[idr < IDR(Y = y, IM, \varepsilon) \text{ in } t \text{ years}] = 1 - \exp\{-v_{IDR}(idr)t\} \tag{2}$$

where Y denotes uncertainties of structural system characteristics (e.g., geometrical dimensions, material parameters, damping characters, etc.), ε represents the uncertainties of ground motion and epistemic uncertainty; $P[idr < IDR(Y = y, IM, \varepsilon)]$ is the probability of structural damage in the design working life.

2.2 Definition of multidimensional performance-based PSDA

In this study, the definition of performance-based PSDA was extended to multi-dimensions to increase the reliability of the structural demand risk assessment. The proposed methodology applies to any EDP, so that the maximum peak floor acceleration (*PFA*) can be also used as an EDP together with the maximum interstorey drift. If the responses *IDR* and *PFA* are used simultaneously and the proposed intensity measurement $S_a(T_1)$ is used as *IM*, the effect of the nonstructural components of the *PFA* on the mean annual frequency of exceedance can be calculated as:

$$v_{IDR,PFA}(idr, pfa) = \int_{IM} P(IDR > idr, PFA > pfa | IM = im) \left| \frac{d\lambda_{IM}(im)}{dim} \right| dim \tag{3}$$

where $P(IDR > idr, PFA > pfa | IM = im)$ represents a two-dimensional hazard fragility function (Cimellaro et al. 2006). Also, $v_{IDR,PFA}(idr, pfa)$ is the mean annual frequency of exceedance that includes two limit states. The uncertainties in both these structural responses are produced by a common source of uncertainties; hence, the two response parameters should be considered to be stochastically dependent using a bivariate lognormal distribution. The two-dimensional probability density function is shown as follows:

$$f(IDR, PFA | IM = im) = \frac{1}{2\pi IDR \times PFA \sigma_{IDR|IM=im} \sigma_{PFA|IM=im} \sqrt{1 - \rho^2}} \times \left\{ \exp - \frac{1}{2(1 - \rho^2)} \times (\alpha^2 - 2\rho\alpha\beta + \beta^2) \right\} \tag{4}$$

where $\alpha = (\ln(IDR) - \mu_{IDR|IM=im}) / \sigma_{IDR|IM=im}$; $\beta = (\ln(PFA) - \mu_{PFA|IM=im}) / \sigma_{PFA|IM=im}$; ρ is the correlation coefficient between $\ln(IDR)$ and $\ln(PFA)$. $\mu_{IDR|IM=im}$ and $\sigma_{IDR|IM=im}$ are the log-mean and the log-standard deviation of interstorey drift, respectively; $\mu_{PFA|IM=im}$ and $\sigma_{PFA|IM=im}$ are the log-mean and the log-standard deviation of peak floor acceleration. The relationship between these two responses and their associated limit states are described using a bidimensional limit state equation. Given this, the probability of exceeding the performance levels can be calculated as

$$P(IDR > idr, PFA > pfa | IM = im) = \int_{idr}^{\infty} \int_{pfa}^{\infty} f(IDR, PFA | IM = im) dIDR dPFA \tag{5}$$

where $f(IDR, PFA | IM = im)$ is a bidimensional lognormal distribution; idr is threshold value of the interstory drift limit state; pfa is threshold value of peak floor acceleration limit state. Substituting Eq. (5) into Eq. (3), we obtain

$$v_{IDR,PFA}(idr, pfa) = \int_{IM}^{\infty} \int_{idr}^{\infty} \int_{pfa}^{\infty} f(IDR, PFA | IM = im) \left| \frac{d\lambda_{IM}(im)}{dim} \right| dIDR dPFA dim \tag{6}$$

From Eq. (6) it can be seen that multidimensional performance-based PSDA requires the computation of two responses and a seismic hazard curve. Equation (6) is calculated using multiple integral trapezoidal methods. If the calculation accuracy and variance reduction are considered, using the trapezoidal method, the computational efficiency will be higher than if the Monte Carlo integral is used (Rahman and Xu 2004; Ming and Zheng 2010; Sun and Pan 2011). The effect of nonstructural components of PFA on the demand hazard curve of the example structure can be calculated as:

$$P[idr < IDR(Y = y, IM, \varepsilon), pfa \text{ in } t \text{ years}] = 1 - \exp\{-v_{IDR,PFA}(idr, pfa)t\} \tag{7}$$

where $P[idr < IDR(Y = y, IM, \varepsilon), pfa]$ is the probability of structural damage that reflects two performance limit states.

2.3 Formulation of multidimensional performance limit state

A generalized MPLSs equation provides a tool for considering dependencies among the threshold vectors of various components. The relationship between various threshold limit states can be determined using the multidimensional surface function (Cimellaro and Reinhorn 2010).

$$L(R_1, \dots, R_n) = \sum_{i=1}^n \left(\frac{R_i}{r_{lim,i}} \right)^{N_i} - 1 = 0 \tag{8}$$

where R_i represents a response parameter (e.g., deformation, acceleration, velocities, etc.), $r_{lim,i}$ represents a response threshold parameter related to structural damage; N_i is an interaction factor determining the shape of multidimensional surface. The two-dimensional and three-dimensional limit state surfaces, which can be generated using the generalized MPLSs equation, are shown in Fig. 2. From Fig. 2a, it can be seen that the dashed line represents the dependency of two-dimensional limit state $r_{lim,1}$ and $r_{lim,2}$. In addition, structural damage will occur if the response parameters fall into the failure domain. Figure 2b represents a relationship between the parameters in the 3D limit state.

For the two-dimensional case, the generalized MPLSs equation can be expressed as follows:

$$\left(\frac{IDR}{idr_{lim}} \right)^{N_{IDR}} + \left(\frac{PFA}{pfa_{lim}} \right)^{N_{PFA}} - 1 = 0 \tag{9}$$

where IDR is the maximum interstory drift; PFA is the maximum peak floor acceleration; idr_{lim} is interstory drift limit state; pfa_{lim} is peak floor acceleration limit state; N_{IDR} and

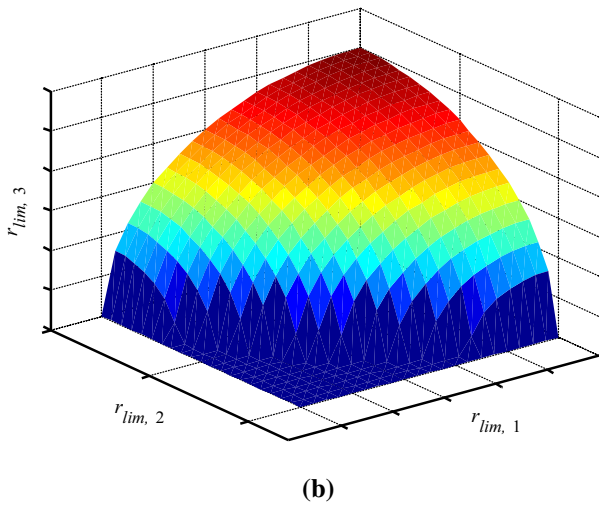
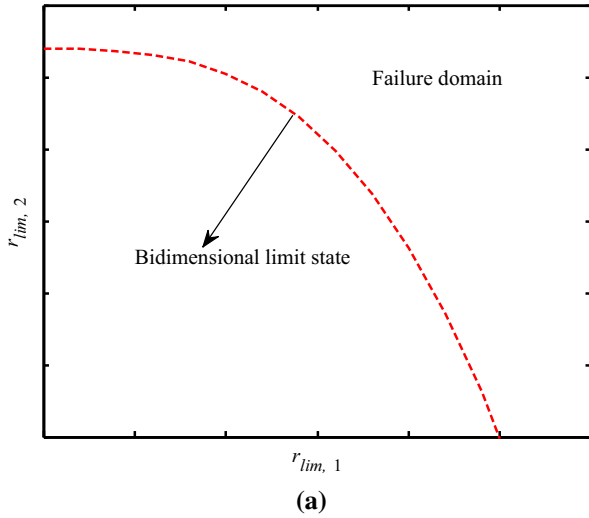


Fig. 2 Multidimensional limit state surface: **a** bidimensional surface; **b** three-dimensional surface

N_{PFA} are interaction factors determining the shape of the surface of two-dimensional limit state.

A simpler expression is obtained by assuming $N_{PFA} = 1$:

$$\frac{PFA}{pfa_{lim}} + \left(\frac{IDR}{idr_{lim}} \right)^{N_{IDR}} - 1 = 0 \tag{10}$$

where idr_{lim} , pfa_{lim} and N_{IDR} are independent quantities and are commonly obtained from field data and probabilistic analysis (Cimellaro and Reinhorn 2010).

3 Effects of uncertainties of limit states

3.1 Different random threshold values for the interstory drift limit state

The performance limit states of structural and nonstructural components represent the level of response and depend on mechanical properties such as strength and deformability, which are, in themselves, uncertain. Consequently, the limit states should be considered to be random variables rather than deterministic quantities. In this section the case is the simplest, where the interstory drift and the associated limit state are treated as random variables and follow a lognormal distribution (Cimellaro et al. 2006). The effects of different random threshold values of the interstory drift limit state on the mean annual frequency of exceedance can be obtained by the following Eq. (11).

$$v_{IDR}(idr_{rand\ lim,i}) = \int_{IM} \int_{\Omega} \int_{idr_{rand\ lim,i}} f(IDR) f(idr_{rand\ lim,i}) \left| \frac{d\lambda_{IM}(im)}{dim} \right| dIDR didr_{rand\ lim,i} dim \tag{11}$$

where Ω is the one-dimensional failure domain of the structure; $f(IDR)$ is the probability density function of the interstory drift; $idr_{rand\ lim,i}$ is a random threshold value of the interstory drift limit state at the i th performance level. $f(idr_{rand\ lim,i})$ is the probability density function (PDF) of interstory drift limit state and is described as follows:

$$f(idr_{rand\ lim,i}) = \frac{1}{idr\sigma_{idr_{rand\ lim,i}}\sqrt{2\pi}} \exp\left\{ \frac{-(\ln(idr_{rand\ lim,i}) - \mu_{idr_{rand\ lim,i}})^2}{2\sigma_{idr_{rand\ lim,i}}^2} \right\} \tag{12}$$

where $\mu_{idr_{rand\ lim,i}}$ and $\sigma_{idr_{rand\ lim,i}}$ are the log-mean and the log-standard deviation of interstory drift limit state at the i th performance level. These two parameters are obtained using Eq. (13):

$$\mu_{idr_{rand\ lim,i}} = \ln(idr_{fixed\ lim,i}), \sigma_{idr_{rand\ lim,i}} = cv \cdot idr_{fixed\ lim,i}, \tag{13}$$

where $idr_{fixed\ lim,i}$ is a deterministic threshold value of the interstory drift limit state at the i th performance level; cv is the coefficient of variation of the random interstory drift limit state.

3.2 Deterministic threshold value of peak floor acceleration limit state

Considering the effect of the deterministic peak floor acceleration limit state, the definition of a mean annual frequency of exceedance is given by the following integral:

$$v_{IDR,PFA}(idr_{lim,ij}, pfa_{lim,j}) = \int_{IM} \int_{idr_{lim,ij}} \int_{pfa_{lim,j}}^{\infty} f(IDR, PFA) \left| \frac{d\lambda_{IM}(im)}{dim} \right| dIDR dPFA dim \tag{14}$$

where $idr_{lim,ij}$ is a deterministic interstory drift limit state at the i th performance level when the effect of j th acceleration threshold is considered; $pfa_{lim,j}$ is the j th fixed peak floor acceleration limit state; $f(IDR, PFA)$ is the bidimensional lognormal distribution. The deterministic threshold values of the interstory drift limit state (0.2–0.5–1.5–2.5 % of story height) is chosen based on FEMA 445 (2006) and four fixed peak floor acceleration thresholds are rooted in ATC58-2 (2006) (0.6 g for the case of immediate occupancy and

1.1 g for the case of collapse prevention). The effects of various deterministic threshold values of the peak floor acceleration on the drift hazard curve can be depicted as (the results are further elaborated in Sect. 5.2):

$$\begin{aligned}
 P[idr_{lim,ij} < IDR(Y = y, IM, \varepsilon), pfa_{lim,j} \text{ in } t \text{ years}] \\
 = 1 - \exp\{-v_{IDR,PFA} v_{IDR,PFA}(idr_{lim,ij}, pfa_{lim,j})t\}
 \end{aligned}
 \tag{15}$$

3.3 Different random threshold values for drift and acceleration limit states

Taking into consideration the two randomly independent limit states and two dependent responses, the mean annual frequency for exceeding two random limit levels can be computed as follows:

$$v_{IDR,PFA}(idr_{rand\ lim,i}, pfa_{rand\ lim,i}) = \int_{IM} \int_{idr_{rand\ lim,i}}^{\infty} \int_{pfa_{rand\ lim,i}}^{\infty} f(IDR, PFA) \left| \frac{d\lambda_{IM}(im)}{dim} \right| dIDR dPFA dim
 \tag{16}$$

where $idr_{rand\ lim,i}$ is a random threshold value of the interstory drift limit state at the i th performance level; $pfa_{rand\ lim,i}$ is a random threshold value for the peak floor acceleration limit state at the i th performance level. Since the PDF of the peak floor acceleration limit state is similar to Eq. (12), the log-mean and the log-standard deviation of the limit parameter can be also expressed as follows:

$$\mu_{pfa_{rand\ lim,i}} = \ln(pfa_{fixed\ lim,i}), \sigma_{pfa_{rand\ lim,i}} = cv \cdot (pfa_{fixed\ lim,i}),
 \tag{17}$$

where $pfa_{fixed\ lim,i}$ is a deterministic threshold value for the peak floor acceleration limit state at the i th performance level; cv is the coefficient of variation for the peak floor acceleration limit state (the same coefficient of variation for both limit states is used in this study).

3.4 Randomly interdependent drift and acceleration thresholds

Here, it is reasonable to assume that the bidimensional failure domain can be defined by the following equation:

$$L(IDR, PFA) = PFA/pfa_{rand\ lim,i} + (IDR/idr_{rand\ lim,i})^{N_{IDR}} \geq 1
 \tag{18}$$

where N_{IDR} determines the dependency between the bidimensional limit states. Different values of the parameter N_{IDR} (e.g., 1, 2, 3, 5 and 15, etc.) were used to determine the sensitivity of the demand hazard curve.

Using the description in Eq. (18), the mean annual frequency of exceeding two randomly interdependent limit levels can be expressed using the following Eq. (19).

$$v_{IDR,PFA}(idr_{rand\ lim,i}, pfa_{rand\ lim,i}) = \int_{IM} \iint_D f(IDR, PFA) \left| \frac{d\lambda_{IM}(im)}{dim} \right| dIDR dPFA dim
 \tag{19}$$

where D is the two-dimensional failure domain denoted by Eq. (18).

4 Case study

4.1 Description of an RC building

To demonstrate the proposed method and provide insights into the impact of uncertainties in the two-dimensional limit states on the drift hazard curve, a sample six story RC frame structure was used as case study example. The elevation of the longitudinal and transverse frames in the building is shown in Fig. 3. The total height of building is 18 m. The lengths of longitudinal and transversal spans were 32 m and 12 m, respectively. Moreover, columns and beams' cross sections were 450 mm \times 450 mm and 300 mm \times 300 mm, respectively. The distributed steel in the building members was calculated using building code GB50011 (2010). Nonstructural components in the modelled RC building were infill walls, which were regularly distributed from second story to the roof (Fig. 3). The designed thickness of the infill walls was 240 mm. The foundation was assumed to be on medium hard soil represented by site class II (the shear wave velocity was between 250 and 500 m/s). The seismic grade of the RC frame structure was level 2 (JGJ3 2010).

4.2 Material parameters of the building components

All members in the modelled building were composed made of RC structural components reinforced HPB335 (longitudinal rebar) and HPB235 (stirrups). The foundation of the building employed C30 concrete with 100 mm of C15 cushion plain concrete. The elasticity modulus of the concrete and steel were 30GPa and 200GPa. Their corresponding Poisson's ratios were 0.2 and 0.3. The density of the reinforced concrete was 2500 kg m⁻³. For the nonstructural components (infill walls), the strength of the brick and mortar were MU10 and M5. The elasticity modulus and the density of the masonry were 2.4GPa and 1900 kg m⁻³ (GB50011 2010).

4.3 Finite-element modeling

A nonlinear dynamic model of the RC building was generated using the finite element analysis software SAP2000. Generally, the M3 hinge, P-M2-M3 hinge and V2 hinge were used to model both ends of the RC columns and beams. The plates were modeled using the

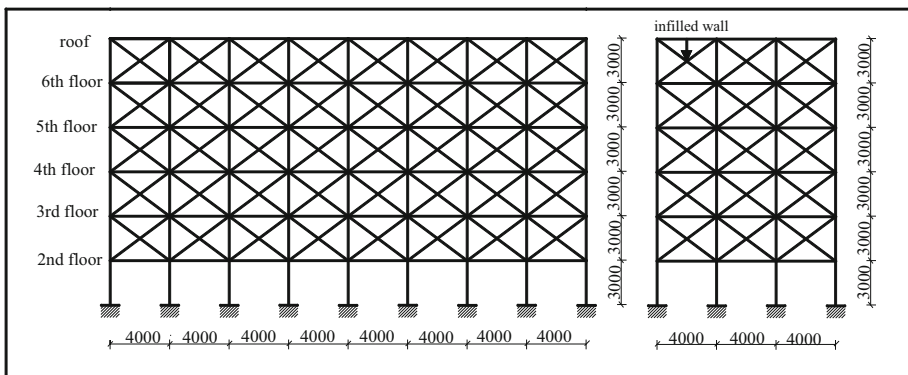


Fig. 3 The elevation of the longitudinal and transverse frames in the building

shell-thin element. The infill walls were assumed to be equivalent to an oblique compression bar, which was modeled using truss element and uniaxial hysteresis materials (Li et al. 2009). The fundamental mode for the given structure was set at 0.6557 s in a small earthquake. A major earthquake was found to initially generate plastic hinges at each end of the beams on the ground floor and second floor of the building. Sequentially, these hinges occurred at the bottom of corner column, which was the concentrated region of structural stress.

4.4 Ground motion input

Ground motion input is an uncertain quantity that can have a significant influence on the evaluation of the structural responses to seismic loading, because it is very difficult to estimate the plethora of possible parameters (e.g., magnitude, spectrum characteristic, duration, etc.) involved in seismic event. Baker and Cornell (2005) illustrated how ground motion records can be selected for a study using the Conditional Mean Spectrum (CMS). In parallel with recent conceptual work (Baker 2010), the target response must be calculated using the seismic effect coefficient curve (GB50011 2010).

An efficient criterion that can be used to match ground motion and the target spectrum (CMS) is the sum of squared errors (*SSE*) between the logarithms of the record's spectrum and the target spectrum, as detailed in the work of Baker (2010)

$$SSE = \sum_{j=1}^n (\ln Sa(T_j) - \ln Sa_{\text{target}}(T_j))^2 \quad (22)$$

where $\ln Sa(T_j)$ is the log of the spectral acceleration of the ground motion at period T_j ; $\ln Sa_{\text{target}}(T_j)$ is the log of the target spectrum value at period T_j . The periods T_j should cover the period range and 50 T_j values per order of magnitude of periods is sufficient to discriminate between ground motion records with a legitimate match to the target spectrum.

Using this process, sixty real earthquake records ($M = 6.5\text{--}6.9$, $R = 0.5\text{--}20$ km) were chosen for capturing the uncertainties of ground motions. Finally, as demonstrated in Fig. 4, twenty actual seismic inputs were selected whose response spectra shapes were similar to the shape of the target response spectrum. In Fig. 4, the dashed line represents the mean response spectrum (damping ratio, $\xi = 5\%$).

4.5 Definition of performance levels and computations of the two maximum responses

The performance levels of the RC building were classified into four grades, normal operation, immediate occupancy, life safety and collapse prevention, according to the combination of the performances between structural components and nonstructural components. The threshold values of both limit states that influence the four performance levels are shown in Table 1 (ATC58-2 2006; FEMA 2006).

Incremental Dynamic Analysis (IDA) is regarded as a novel approach that provides a relationship between the intensity measurement and the seismic response (Vamvatsikos and Cornell 2002, 2004). To perform a complete range of the structural response from elasticity to finally collapse, a series of twenty selected recorded ground motions were entered into the FE model. Each record was scaled from low *IM* levels to higher *IM* levels until a structural collapse occurred. Figure 5 shows the twenty IDA curves of $S_a(T_1)$ versus

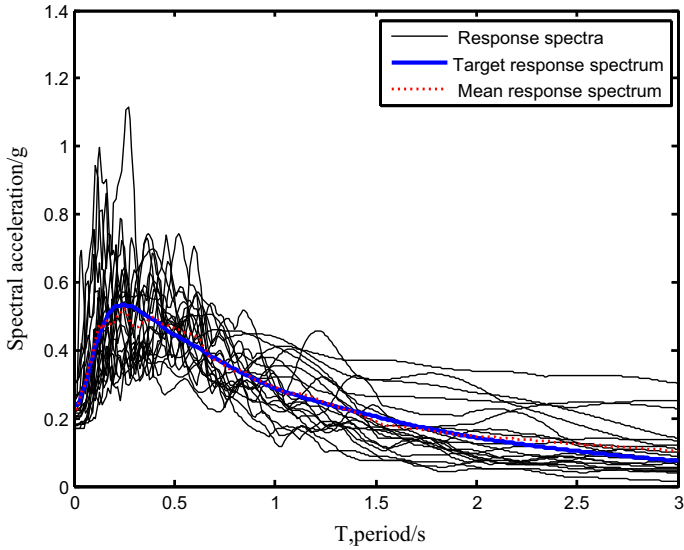


Fig. 4 Response spectra of ground motion records

Table 1 The threshold values of interstory drift and peak floor acceleration limit states

Four performance levels	Normal operation (NO)	Immediate occupancy (IO)	Life safety (LF)	Collapse prevention (CP)
$idr_{fixedlim,i}$ (%)	0.2	0.5	1.5	2.5
$pfa_{fixedlim,i}$	0.4 g	0.6 g	0.8 g	1.1 g

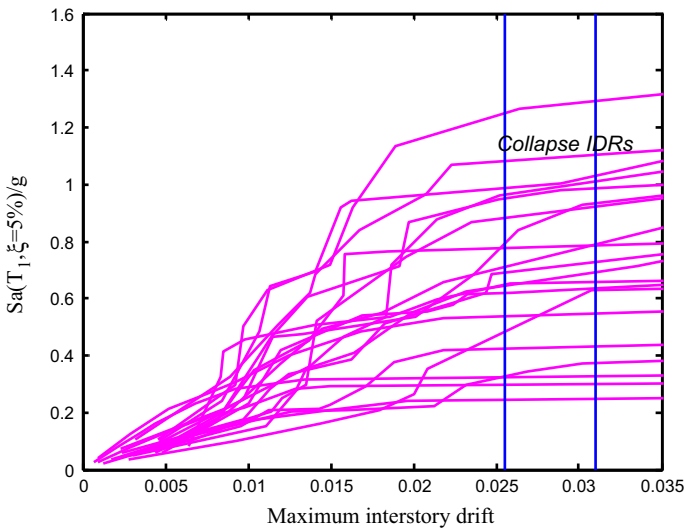


Fig. 5 Twenty IDA curves of $S_d(T_1)$ versus interstory drift

interstory drift. The collapsed interstory drift is acquired when each IDA curve is close to horizontal line. Moreover, the maximum accelerations of the nonstructural components (infill walls) were calculated using nonlinear time history analysis. Similarly, all of the chosen earthquake records were scaled to different intensity levels. In general, the collapse of the nonstructural components will occur if the maximum peak floor acceleration exceeds 1.1 g (Sun et al. 2013).

4.6 Seismic hazard

The geographical location of the modelled building is designated to be western China. This was a Class II site, with eight times the intensity of an earthquake and the designing ground acceleration was set as 0.20. Employing these parameters, the seismic hazard analysis was conducted using the simplified model (Jalayer 2003; Cornell and Krawinkler 2000) shown below:

$$\lambda_{S_a}(S_a) = P[S_a \geq x] = k_0 \cdot x^{-k_1} \quad (22)$$

where $\lambda_{S_a}(S_a)$ is the mean annual frequency of exceeding a given intensity measure, k_0 is a constant related to the ground motion characteristics and k_1 is the slope of the seismic hazard curve in logarithmic coordinates. Since the mean annual frequencies of medium and major earthquakes are 1/1475.475 and 1/12,475.2475, respectively, k_0 and k_1 can be calculated through the interpolation of two known points. Here, $k_0 = 0.000079203$ and $k_1 = 2.3814$.

5 Sensitivity analysis on drift hazard curves

5.1 Effects of different random threshold values of the interstory drift limit state

A sensitivity analysis of the coefficient of variation was necessary, because the interstory drift hazard curve is affected by the various random threshold values of interstory drift limit state. Figure 6 shows the effects of the different values of the coefficient of variation on the drift hazard curve. As can be seen from Fig. 6, the differences between the drift hazard curves corresponding to $cv = 0.1$ as well as $cv = 0.5$ and $cv = 1.0$ are quite small. However, the drift hazard curve with a limit state uncertainty of $cv = 0$ is lower than the others which signifies its importance to the limit state uncertainty. For collapse prevention level, it is observed that the drift hazard curve with a deterministic limit state is less than 33 % of the others with the limit state uncertainty. This indicates that the use of random threshold values for the drift limit state can produce conservative results in contrast to results based on the deterministic threshold value.

5.2 Effects of different deterministic threshold values of peak floor acceleration

A significant study reported by Cimellaro and Reinhorn (2010) concluded that the threshold values of the peak floor acceleration limit state are not stable. As a result, the drift hazard curve was investigated, where the deterministic threshold of the interstory drift limit state was fixed, while the threshold value of the peak floor acceleration varied from

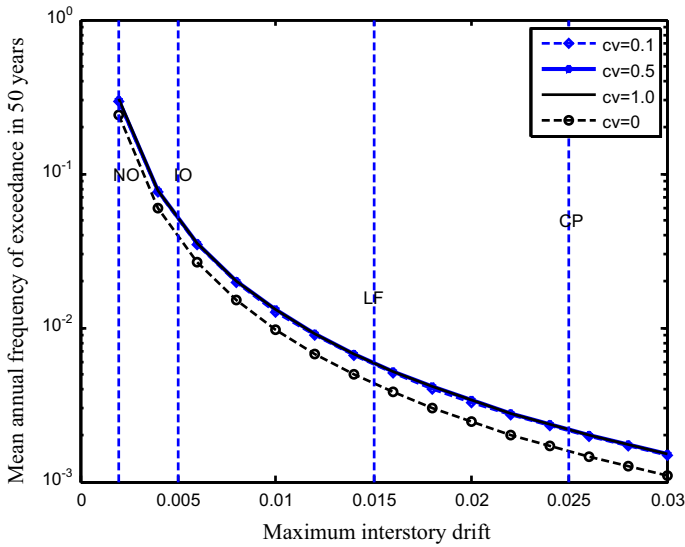


Fig. 6 Effects of the different values of the coefficient of variation on the drift hazard curve

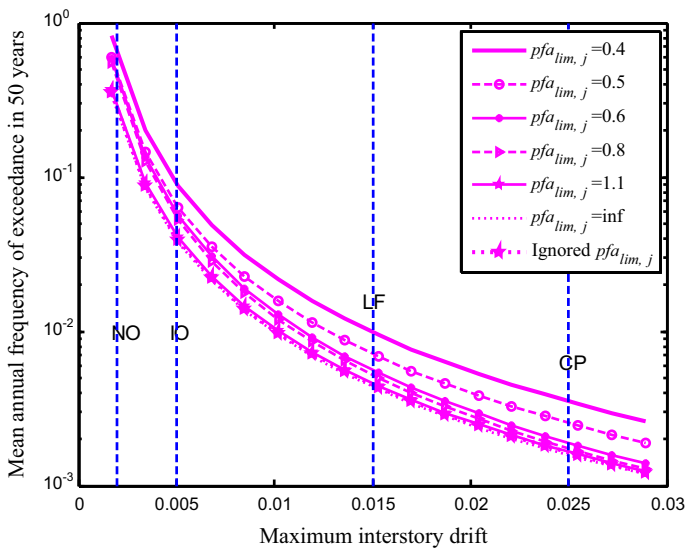


Fig. 7 Drift hazard curves based on different threshold values of the peak floor acceleration limit state

0.4 g to ∞ . For comparison, the drift hazard curves based on different threshold values of the peak floor acceleration limit state are shown in Fig. 7. As can be seen in this figure the sensitivity of the acceleration threshold values will be reduced if the threshold value is greater than 0.8 g. However, the drift hazard curve that ignores the acceleration threshold is smaller than that the one that reflects acceleration threshold values of $pfa_{lim} = 0.4$ and $pfa_{lim} = 0.5$. The results shown in Fig. 7 demonstrate that the mean annual frequency of

exceedance will be underestimated if the threshold value of the acceleration limit state is not chosen accurately.

5.3 Effects of different random threshold values of two limit states

In this section, the same coefficient of variation for both limit states was applied to perform the sensitivity analysis of the drift hazard curve when two randomly independent limit states were introduced. The drift hazard curves, which are built for different values of the coefficient of variation related to the limit thresholds, are plotted in Fig. 8. From the drift hazard curves at the life safety and collapse prevention performance levels, it can be seen that the mean annual frequency of exceedance will be underestimated if the uncertainties of the two limit states are neglected ($cv = 0$). However, the computation results will be more conservative if the coefficient of variation is suitably increased. The mean annual frequency of exceedance described in Eq. (16) at the normal operation performance level is 0.14711 as defined by the Monte Carlo integral (10^5 times). Considering the variance reduction, Monte Carlo cannot provide the approximate distribution. If the integral dimension is less than four, the computational efficiency employing the trapezoidal method will be much better than it would be using the Monte Carlo method (Rahman and Xu 2004; Ming and Zheng 2010; Sun and Pan 2011).

5.4 Effects of randomly interdependent drift and acceleration limit states

The parameter N_{IDR} describes the shape of two-dimensional limit states. The relationship between the two limit states becomes a regular/irregular arc-shaped, when $N_{IDR} \geq 2$. If $N_{IDR} \rightarrow \infty$, the limit states of interstory drift and peak floor acceleration are not correlated. Figure 9 shows the influence of different values on the parameter N_{IDR} on the drift hazard curve. The data in this figure show that the drift hazard curve will be relatively

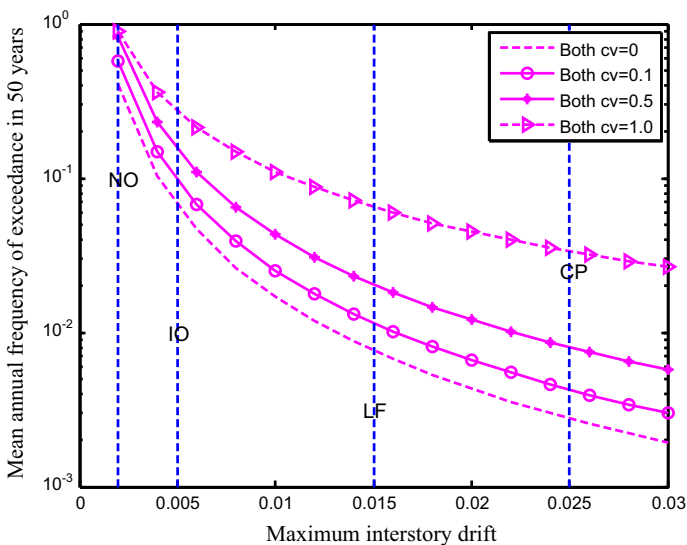


Fig. 8 Drift hazard curves based on different threshold values of both the limit states

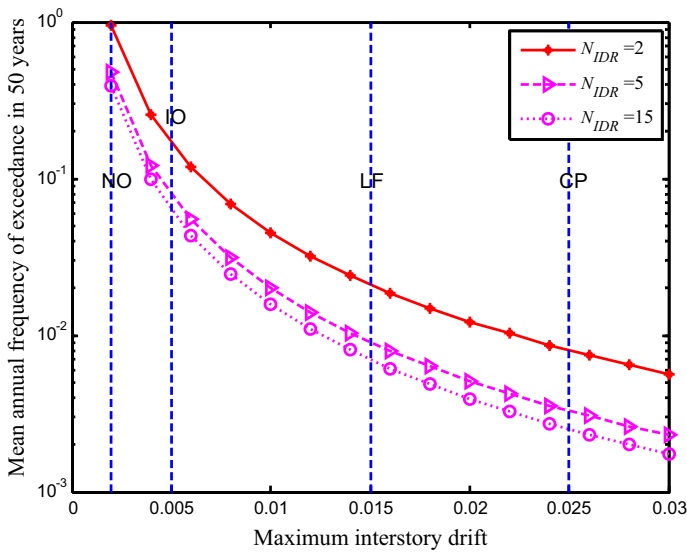


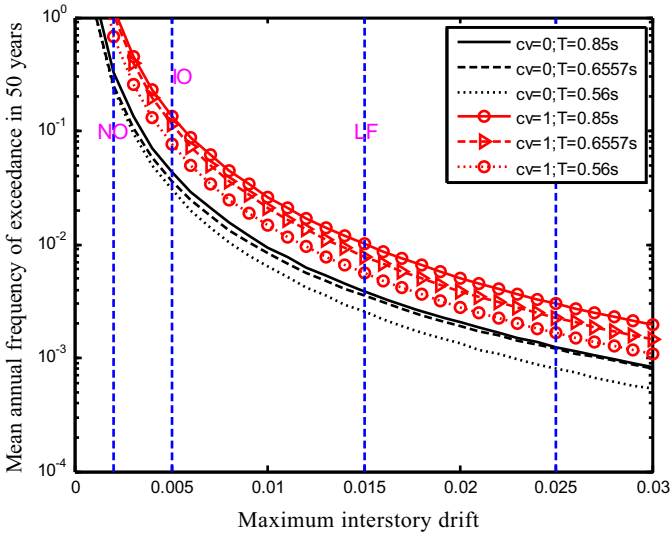
Fig. 9 Influence of different values on the parameter N_{IDR} on the drift hazard curve

conservative if the value of the parameter N_{IDR} is selectively assigned. For example, the drift hazard curve corresponding to $N_{IDR} = 2$ are quite difference from the drift hazard curve corresponding to $N_{IDR} = 15$. It is observed that differences may up to 66.9 % for life safety performance level. Normally, the dependency between the two limit states is continually reduced as the value of the parameter N_{IDR} is increased.

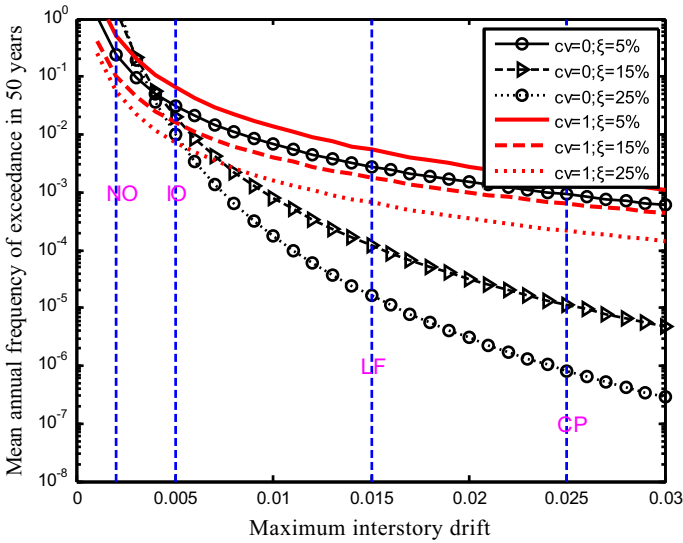
5.5 Sensitivity of the drift hazard curves to structural parameters

Recent reports (Cimellaro et al. 2006; Cimellaro 2007; Cimellaro et al. 2009) have stressed that it was essential to consider the effects of structural parameters (e.g., stiffness, damping and strength, etc.) in a structural risk assessment to ensure the reliability of the results. Figure 10a shows the influence of stiffness on the drift hazard curve and how increments of stiffness reduce the mean annual frequency of exceedance. From this figure, it can be seen that the uncertainties in the limit states generate large values of the mean annual frequency of exceedance and a reduction in this parameter can be realized by stiffening the structure. This revelations lead to the conclusion that if uncertainties in the limit states are omitted, the structural risk assessment may be inaccurate.

Some earlier reported work (Barron-Corverra 2000; Reinhorn et al. 2001) has highlighted that additional damping can play a significant role in the evaluation of structural reliability. The drift hazard curves for numerous values of damping ratios (5, 15 and 25 %) are plotted in Fig. 10b. As shown, a drastically reduction in the mean annual frequency of exceedance can be obtained for IDR values of up to 0.41 %, when damping ratio is increased [Fig. 10b]. However, this reduction is not proportional to additional damping. It is observed in Fig. 10b that not considering uncertainties in the limit states can be non-conservative for drift values of up to 0.8 %, depending on the level of damping considered, and conservative for lower drift values. Other structural parameters, such as strength have also been considered. But increments of strength do not produce significant improvements



(a)



(b)

Fig. 10 Effects of **a** increased stiffness; **b** additional damping when the uncertainties of limit states are included

in drift hazards, since the inelastic displacement might not be distinctly affected by changes in strength. In summary, the influence of strength, stiffness, and damping may be used in decisions about the use of retrofitting techniques.

6 Conclusions

In this reported study, the definition of performance-based PSDA was primarily extended to include multi-dimensions. A nonlinear model of a six story RC building was established to verify the proposed analysis method. The maximum interstory drift of the modelled structure was calculated using IDA and the maximum peak floor acceleration of infill walls was attained using a nonlinear time analysis. The two response variables were considered to be dependent and were described by a bivariate lognormal distribution. The relationship between the two demand responses and their associated limit states was defined using a generalized MPLSs equation. The drift hazard curve for the structure was developed by combining the bivariate PDF and the seismic hazard curve.

From the proposed numerical analysis, it can be concluded that the uncertainties in the two limit states for the modelled structure contribute positively to the seismic demand risk assessment of the structure, particularly when comparing various structural retrofitting techniques. If the coefficients of variation, peak floor acceleration threshold and the interaction factor N_{IDR} are suitably chosen, the drift hazard curve will be relatively conservative. Furthermore, parametric analyses illustrated that additional structural damping had a considerable effect on the drift hazards from the perspective of increased stiffness. The effect of uncertainties in the limit states can effectively resist a reduction in the mean annual frequency of exceedance when damping ratio is increased.

Since PEER's PBEE approach involves four stages: hazard analysis, structural analysis, damage analysis, and loss analysis (Porter 2003), the proposed methodology, termed damage analysis, may be useful for future economic loss evaluation.

Acknowledgments The research support from the National Natural Science Foundation of China (51278420) and Graduate Starting Seed Fund of Northwestern Polytechnical University (Z2014114) were greatly appreciated.

References

- ATC58-2 (2006). Preliminary evaluation of methods for defining performance, FEMA, Washington D.C of USA
- Baker JW (2010) Conditional mean spectrum: tool for ground-motion selection. *J Struct Eng* 137(3):322–331
- Baker JW, Cornell AC (2005) A vector-valued ground motion intensity measure consisting of spectral acceleration and epsilon. *Earthquake Eng Struct Dynam* 34(10):1193–1217
- Barron-Corverra R (2000) Spectral evaluation of seismic fragility of structures. PhD Dissertation, State University of New York at Buffalo
- Cimellaro GP (2007) Simultaneous stiffness–damping optimization of structures with respect to acceleration, displacement and base shear. *Eng Struct* 29(11):2853–2870
- Cimellaro GP, Reinhorn A (2010) Multidimensional performance limit state for hazard fragility functions. *Journal of engineering mechanics* 137(1):47–60
- Cimellaro GP, Reinhorn AM, Bruneau M, Rutenberg A (2006) Multi-dimensional fragility of structures: formulation and evaluation, Multidisciplinary Center for Earthquake Engineering Research, University at Buffalo, State University of New York
- Cimellaro GP, Lavan O, Reinhorn AM (2009) Design of passive systems for control of inelastic structures. *Earthquake Eng Struct Dynam* 38(6):783–804
- Cornell CA (1968) Engineering seismic risk analysis. *Bull Seismol Soc Am* 58(5):1583–1606
- Cornell CA, Krawinkler H (2000) Progress and challenges in seismic performance assessment. *PEER Center News* 3(2):1–3
- Deierlein GG, Krawinkler H, Cornell CA (2003) A framework for performance-based earthquake engineering. In: Pacific conference on earthquake engineering, pp 1–8

- FEMA (2006) 445. Next-Generation Performance-Based Seismic Design Guidelines Program Plan for New and Existing Buildings. Prepared by ATC for FEMA, Washington DC
- GB50011 (2010) Code for seismic design of buildings. China Architecture Industry Press, Beijing of China
- Ghobarah A (2001) Performance-based design in earthquake engineering: state of development. *Eng Struct* 23(8):878–884
- Jalayer F (2003) Direct probabilistic seismic analysis: Implementing non-linear dynamic assessments. PhD Dissertation., Stanford University, Ann Arbor
- JGJ3 (2010) Technical specification for concrete structures of tall building. China Architecture Industry Press, Beijing of China
- Kiureghian AD (2005) Non-ergodicity and PEER's framework formula. *Earthquake Eng Struct Dynam* 34(13):1643–1652
- Li Y, Han J, Tian Q, Chen W, Zhao S (2009) Study on influence of infilled walls on seismic performance of RC frame structures. *Journal of Earthquake Engineering and Engineering Vibration* 3:008
- Lin L, Naumoski N, Saatcioglu M, Foo S (2011) Improved intensity measures for probabilistic seismic demand analysis. part 2: application of the improved intensity measures. *Can J Civ Eng* 38(1):89–99
- Ming WY, Zheng HS (2010) Two New Kinds of Monte-Carlo Methods for Solving Numerical Integration. *Math Practice Theory* 10:027
- Moehle J, Deierlein GG (2004) A framework methodology for performance-based earthquake engineering. In: 13th World conference on earthquake engineering, pp 3812–3814
- Porter KA (2003) An overview of PEER's performance-based earthquake engineering methodology. In: Proceedings of 9th international conference on applications of statistics and probability in civil engineering, San Francisco, California
- Priestley MJN (2000) Performance based seismic design. *Bulletin of the New Zealand society for earthquake engineering* 3(3):325–346
- Rahman S, Heqin X (2004) A univariate dimension-reduction method for multi-dimensional integration in stochastic mechanics. *Probab Eng Mech* 19(4):393–408
- Reinhorn A, Barron-Corverra R, Ayala A (2001) Spectral evaluation of seismic fragility of structures. In: Proc., Proceedings ICOSSAR
- Shome N (1999) Probabilistic seismic demand analysis of nonlinear structures. 9924607 Ph.D., Stanford University, Ann Arbor
- Sun F, Pan Z (2011) The extrapolation algorithms for numerical triple integrals. *Numerical Mathematics A Journal of Chinese Universities* 4:010
- Sun HB, Wu ZY, Liu XX (2013) Multidimensional performance limit state for structural fragility estimation. *Eng Mech* 30(5):147–152
- Tothong P (2007) Probabilistic seismic demand analysis using advanced ground motion intensity measures, attenuation relationships, and near-fault effects. PhD Dissertation., Stanford University, Ann Arbor
- Tothong P, Cornell CA (2006) Application of nonlinear static analyses to probabilistic seismic demand analysis. In: Proceedings of 8th US National Conference on Earthquake Engineering 2006, April 18, 2006–April 22, 2006, Earthquake Engineering Research Institute, pp 4373–4382
- Vamvatsikos D, Cornell CA (2002) Incremental dynamic analysis. *Earthquake Eng Struct Dynam* 31(3):491–514
- Vamvatsikos D, Cornell CA (2004) Applied incremental dynamic analysis. *Earthquake Spectra* 20(2):523–553
- Wang QA, Wu ZY, Liu SK (2012) Seismic fragility analysis of highway bridges considering multi-dimensional performance limit state. *Earthquake Engineering and Engineering Vibration* 11(2):185–193
- Wu QY, Zhu HP, Fan J, Zeng ZH (2012) Seismic performance assessment on some frame structure. *J Vib Shock* 31(15):158–164
- Yun S-Y, Hamburger RO, Cornell CA, Foutch DA (2002) Seismic performance evaluation for steel moment frames. *J Struct Eng* 128(4):534–545
- Zeng ZH, Fan J, Yu QQ (2012) Performance-based probabilistic seismic demand analysis of bridge structures. *Eng Mech* 29(3):156–162